VELOCITY MEASUREMENTS UNDER BROKEN WAVES AND BORES

SANDRO LONGO

Department of Civil Engineering, University of Parma, Parco Area delle Scienze 181/A Parma, 43100, Italy

MARCO PETTI

Dip. di Georisorse e Territorio, University of Udine, Via del Cotonificio, 114 Udine, 33100, Italy

The wave dynamics after breaking is widely investigated also because it controls several phenomena in the surf zone and in the swash zone. Measurements are difficult because of the complex and multi-phase structure of the flow. In order to overcome the limitation of the traditional techniques, a set of experiments were carried out in a flume using Doppler Ultrasonic Technique for fluid velocity measurements. The data have been analysed to obtain the fluid velocity at different phase, the mean fluid velocity and bottom stress. Also classical LDA data were collected and analysed using the Hilbert Huang Transform (HHT).

1. Introduction

The wave dynamics after breaking is widely investigated also because it controls several phenomena in the surf zone and in the swash zone. Several numerical models based essentially on non linear shallow water equations (NLSWE) have been developed, but all them need a model for turbulence in the bore. Many authors have measured fluid velocity in bores using Laser Doppler Anemometry (LDA), Hot Wire and Hot Film anemometry, Particle Image Velocimetry (PIV) with good results and with several limitations essentially due to air bubbles.

The aim of the present work is (1) to use a recent technique for analysing strongly non-linear signals as those collected using LDA in a pre-breaking section of waves; (2) to use Ultrasound Doppler Velocity Profiler data for fluid velocity and bottom friction estimation in a breaking wave and in a bore. These last measurements are rarely available, because of the difficulty in measuring fluid velocity in a strongly aerated flow field.

The results will improve flow field modelling under breaking waves and bores.

2. The experiments

The present analysis refers to experiments on spilling breakers in a wave flume, with Laser Doppler Anemometry and UltraSounds measurements taken in the pre-breaking section and in the bore moving region. The experiments were carried out in the small flume in the laboratory of the Ocean and Coastal Research Group at the Universidad de Cantabria in Santander, Spain. The flume is 24 m long, 0.58 wide and 0.8 m deep and has glass side-walls and bottom (Figure 1).

The wave generator has a paddle with an active absorption system in use to correct for long waves in the channel. A false Plexiglas bottom was installed in the wave flume, creating a uniform slope 1:20 starting 8.0 m from the paddle. The slope has been sealed to the flume walls filling the gap between the edges of the slope and the side walls with silicone.

The local wave height was measured using capacitance wave gauges. A 2-D Laser Doppler Velocimeter was used for velocity measurements. This was a back-scatter, four-beams system with a 6 W ion-argon laser generator refrigerated by water. A 30.00 m optical fiber carried laser beams from an optical system to the measurements location, where it was fixed into a two dimensional programmable transverse system. The Doppler frequency information was elaborated by a counter and stored in a PC. The expected error in velocity measurements was 1% of the velocity range. The test refers to a 5th-order regular wave having period equal to $T = 3.0$ s and height $H = 10$ cm with a s.w.l. in front of the paddle equal to 37 cm. The wave was breaking as a spiller.

Velocity measurements were carried out in 21 points in the vertical of a single section at 13.0 m from the paddle in the sloping bottom part of the tank, with a still water level $h = 12$ cm. The section of measurements was just before the breaking, in order to limit the air bubbles content and to allow also for LDV measurements over a portion of the wave crest. The water was added with TiO_2 tracer which was specifically chosen to improve UltraSounds S/N ratio and not LDA S/N ratio. The first measurement point was the nearest to the bottom. Other points of measurement were equally spaced at 10 mm along the vertical. Only 19 of these point measurements were suitable for further analysis, which covers more than half of the crest. The measurements lasted for 300 s at each level (100 wave cycles) with a data rate variable during the wave period because related to the number of validated bursts per unit time, which was varying. In order to obtain time series with a constant time step, the data was linearly interpolated at 2 kHz, which is ~20% higher than the mean frequency acquisition data rate. In the average the response of the system is satisfactory up to 1.6 kHz. More details on experiments are reported in Longo et al. (2001).

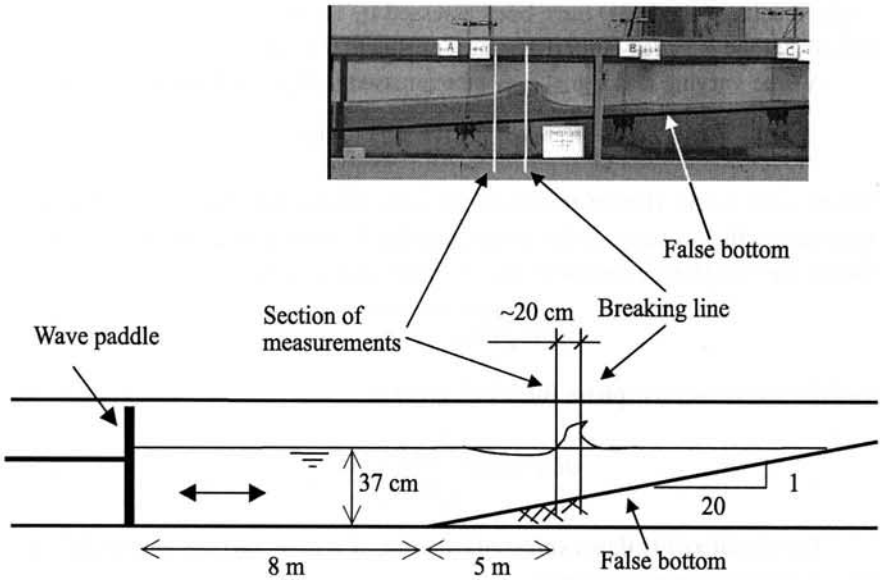

Figure 1. Layout of the flume.

In a second series of tests measurements were carried out using UltraSound probes in Section A and in Section B. In each Section, three Ultrasonic transducers were affixed below the false bottom, the middle being perpendicular to it and the other two at ± 20° respect to the normal.

Each transducer measures the axial velocity component as a function of the axial position. To investigate a 2-D flow fields, two probes are strictly necessary and the third can be used to estimate the errors. The transducers have a plastic housing 18 mm in diameter and active element diameter of 14 mm, with a carrier frequency of 1 MHz and a near field (a region starting near the probe with amplitude modulation of the intensity of the sonic field along the axis; it is suggested to avoid measurements in this region) extending for 32 mm, with a divergence angle in the far field equal to ~ 7.5°. With the adopted set-up, the frequency of acquisition is of ~ 30 profiles/s per probe. A total of 5000 profiles for each test and in each section were recorded for later analysis.

3. Measurements with LDA

A suitable tool for analysing complicate multi-scale non-linear signal is called Empirical Mode Decomposition (EMD). EMD and the Hilbert transform applied

to the results of the EMD have been assessed by Huang et al. (1998) and, hence, this technique is called Hilbert-Huang Transform (HHT).

A time-varying real signal may be expressed in the canonical representation

$$Z(t) = A(t)\exp\left[i\phi(t)\right] = x(t) + i\tilde{x}(t) \qquad (1)$$

where $\tilde{x}(t)$ is the Hilbert transform of $x(t)$. Essentially the Hilbert transform emphasises the property of the function at the location time t. From $Z(t)$ one can define the "magnitude function" (or envelope signal) $A(t)$ as

$$A(t) = \sqrt{x^2(t) + \tilde{x}^2(t)} \qquad (2)$$

and the instantaneous "phase function" $\phi(t)$ as

$$\phi(t) = \tan^{-1}\left[\frac{\tilde{x}(t)}{x(t)}\right] \qquad (3)$$

The signal $x(t)$ is thus expressed in terms of a time-varying amplitude and a time-varying frequency given by

$$f(t) = \frac{1}{2\pi}\frac{d\phi(t)}{dt} \qquad (4)$$

The time-varying frequency is always admissible from a mathematical point of view, but in order to have a physical meaning the source function must: (1) be symmetric with respect to the local zero mean, (2) have the same numbers of zero crossing and extrema. The first condition is equivalent to the traditional "narrow band requirements" for a stationary Gaussian process, the second condition is a surrogate for the requirement of a local mean being zero; the definition of a local mean requires a local time scale evaluation, which is obviously non-objective. The mean of the envelope of the maxima and of the minima of the source signal is a much more objective definition. In order to satisfy these two needs, the source signal has to be decomposed in a set of functions called Intrinsic Mode Functions (IMF). EMD is a numerical tool to extract IMFs from the signal.

The method has been applied to the velocity and free surface measurements already described. In the present experiments the average data rate is equal to 1.6 kHz and the maximum instantaneous frequency detected using HHT for fluid velocity is equal to ~ 400 Hz. The maximum frequency is considerably reduced for the instantaneous water level signal, due to the physics of the interface and to the limited cut-off frequency of the transducers, and assumes a value of ~ 20 Hz.

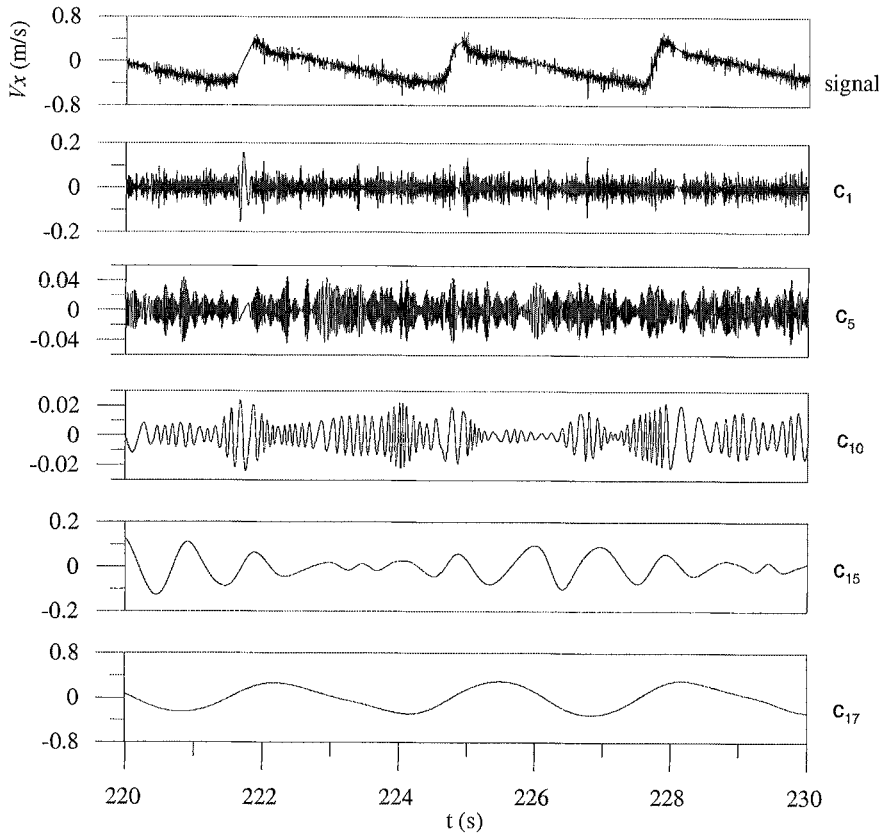

Figure 2. Huang empirical decomposition in IMFs for the fluid velocity signal measured at z = 10 mm from the bottom. The component c_{17} has mean period equal to the regular wave period.

In the average the signal decomposition of the fluid velocity requires more than twenty IMF. In Figure 2 are reported some IMFs for the V_x measurements taken at 10 mm from the bottom.

The relationships between the free surface and the fluid velocity have been analysed by computing the correlation coefficient function amongst the IMFs. Considering the i-IMF of the free surface level and the j-IMF of the fluid horizontal velocity

$$\begin{aligned} \eta(t) &= c_i(t) \\ u(t) &= c_j(t) \end{aligned} \qquad (5)$$

the correlation coefficient function is computed as

$$\rho_{u\eta}(\tau)=\frac{R_{u\eta}(\tau)-(\bar{u})(\bar{\eta})}{\sqrt{\left[R_{uu}(0)-(\bar{u})^2\right]\left[R_{\eta\eta}(0)-(\bar{\eta})^2\right]}} \quad (6)$$

where $R_{u\eta}$ is the cross-correlation function and the overbar indicates the mean value. The shaded contour map of the maximum correlation coefficient vs. frequency is shown in Figure 3.

The cross lines shaded area refer to unphysical frequencies in the free surface spectrum, limited by the probes at ~ 20 Hz. A significant peak corresponds to the forcing frequency at 0.33 Hz, with two secondary peaks along the diagonal, almost symmetric (in log-log plot) with respect to the main peak. High values of the correlation coefficient are also detected at low frequencies, but they have minor relevance due to the low energy contained at such frequencies. A similar plot for the vertical fluid velocity at the same level reveals still high values at low frequency and two maxima (peaks A and B) near the forcing frequency. The peak A is located at twice the forcing frequency. Peak C accounts for high correlation between free surface fluctuations at ~ 15 Hz and horizontal fluid velocity fluctuations at ~ 3 Hz.

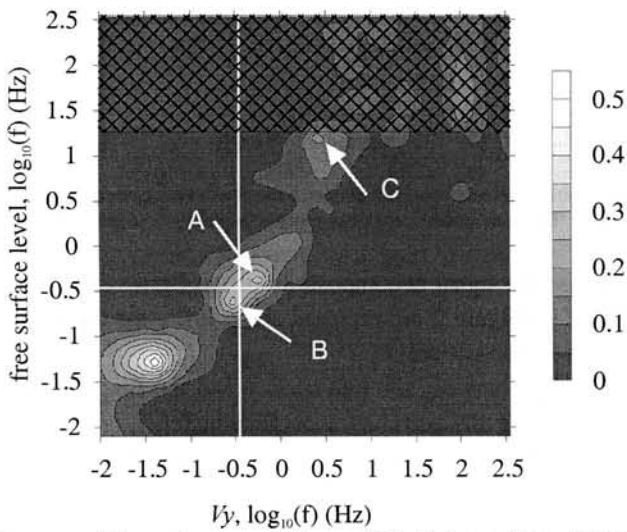

Figure 3. Contour map of the maximum correlation coefficient between free surface level measurements and vertical fluid velocity. Velocity measurements at z = 10 mm.

4. Measurements with Ultrasound Doppler Velocity Profiler (UDVP)

In locating the volume of measurements in UDVP measurements, it is necessary to consider that the ultrasonic beam passing through plexiglass modify its path, due to refraction in the medium having different acoustic impedance. The first useful point of measurement is near the false bottom and measurements extend for 126 spatial positions (gates) along the US probe axis. The measuring volume of a single gate is a disk having a thickness of $h = 1.5$ mm and a radius progressively increasing starting from 7 mm. The velocity components in x and y directions and the variances can be obtained measuring velocity components along the beam axes.

The two main source of errors are the Doppler noise and the presence of air bubbles. Multiple particles or micro eddies present in the volume of measurement scatter echoes broadening the spectral peak. Some tests conducted by Nikora & Goring, 1998, indicate that Doppler noise is essentially a Gaussian white noise; Doppler noise depends on the seeding particles, and is higher in presence of bubbles. Several tests were carried out in order to evaluate the effects of the bubbles (Longo, submitted). Experiments and analysis of results show that measurements of velocity using ultrasound Doppler based velocimeters in a two-phase stationary flow field (air or Hydrogen bubbles and water) give substantially the velocity of the bubbles. This effect is independent of the void bubble volume fraction and still applies to micrometry hydrogen bubbles. In most practical situations (bubble volume fraction < 0.1) the UltraSound celerity is unaffected by bubble presence and the celerity in pure water can be adopted with negligible error. All the above mentioned results are valid in the range 1-10 MHz of the UltraSound carrier.

Due to the intrinsic nature of bubbly flows, the STD of the measured velocity is relatively high and is not a good indicator of turbulence energy.

4.1. *Mean velocity*

The ensemble average horizontal velocity in the bore section for the $T = 3.0$ s wave are shown in Figure 4. The bore profile is reported in the inserted panel.

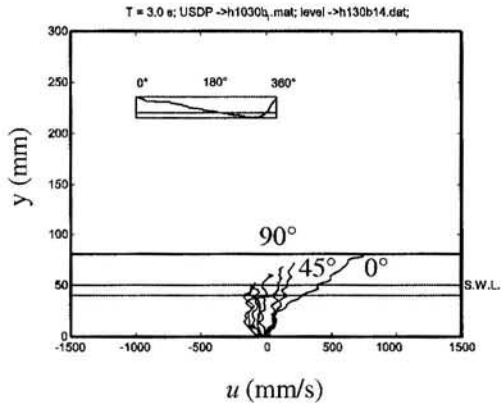

Figure 4. Measured horizontal velocity in the bore at different phases. $T = 3.0$ s.

In order to check the reliability of our measurements, we started to verify mass balance in a period. It is well known that on a long straight coast with uniform longshore condition, or in a flume, the cross shore mass flux must be zero, even though a circulation is associated due to the flux in the crest, especially in presence of breaking. The offshore current below the mean water level is the classical undertow and compensates for the mass flux of the waves. In all tests the error in mass of water is less than 3% of the mass transferred shore-ward (or sea-ward) during the half-cycle. Part of this mass flux is due to bubble presence (which are recorded as water mass by the instrument), part is due to the unavoidable 3-D effects and to the errors in the measurement technique. The time average and the phasic average velocity in the vertical for the 2.5s wave are shown in Figure 5. The velocity is non-dimensional respect to the wave crest celerity and the water depth is non-dimensional respect to the still water level. The profiles are similar in the two sections, with a mean value smaller than 0.1.

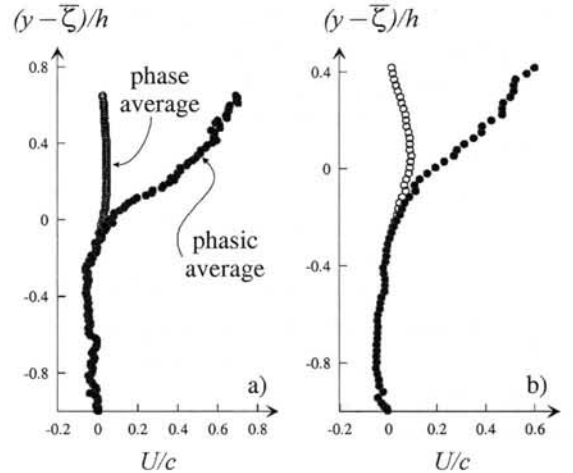

Figure 5. Phase average and phasic average of the velocity profile in the breaker (a) and in the bore (b). Velocity is non-dimensional respect to wave celerity. $\overline{\zeta}$ is the mean water level and h is the still water level. $T = 2.5$ s.

4.2. *Bottom boundary layer*

In order to obtain the wall stress using velocity profile near the bottom, we used the signal of one of the two inclined probes. In fact very close to the bottom, in the boundary layer, the vertical velocity component is negligible and most information is carried out by the horizontal velocity component. Using a single probe has also the advantage that the co-ordinate transformation and the vector composition are not necessary, gaining an improvement of the overall accuracy.

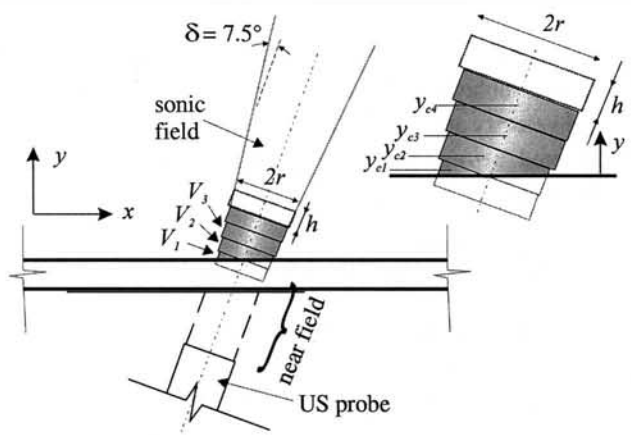

Figure 6. Characteristics of the measurement volume near the bottom.

The volume of measurement at each gate can be roughly considered as a disk of radius r (increasing with distance from the probe) and height h, but if it intersects the wall, only the part of the volume in the flow field is active. As a consequence while the gates far from the bottom are equally spaced at a relative distance h (in the US axis direction), the first gates (*yc1* and *yc2* in Figure 6) are unequally spaced and very near to the bottom. It is a strong advantage because it represents an increment of spatial resolution in the zone where we need it in order to evaluate the bottom stress.

Assuming that there are enough particles equally distributed in the volume of measurements to guarantee an uniform energy scattering, and that the sonic field is almost uniform, Kikura et al. (2004) give the following estimation accurate to first order of the mean velocity in the mass center point of the volume completely immersed in the fluid:

$$\overline{u_\theta}(y_c) = \langle u_\theta \rangle - G(\theta, h, r) \left. \frac{\partial^2 \overline{u_\theta}}{\partial y^2} \right|_{y_c} \qquad (7)$$

with θ the US probe axis inclination to the horizontal. The operator <...> stands for ensemble average, assumed equal to the velocity signal of the instrument. The correction is more cumbersome for those cases with the volume of measurements intersecting the wall. Similar corrections are available for the Reynolds stress. Both the wall distance and the phase averaged measured velocity, projected parallel to the bottom, are normalized with the inner variables, i.e. the viscosity length scale ν/u_* and the wall shear stress velocity u_*:

$$y^+ = \frac{y u_*}{\nu}, \; u^+ = \frac{u}{u_*}, \; u_* = \sqrt{\frac{\tau_b}{\rho}}, \qquad (8)$$

where ρ is the mass density of the fluid. The velocity profile is expected to be linear in the viscous sublayer ($0 < y^+ < 8$) and at a first order the mean velocity and the ensemble velocity are coincident.

For the adopted set-up, the velocity profile in the viscous sublayer is expressed by the following relation

$$\langle u_{\theta i} \rangle = \frac{\cos\theta u_*^2}{\nu} y_i \equiv a y_i \text{ for } i = 1, 2, ..., n \qquad (9)$$

The experimental values $(\langle u_{\theta i} \rangle, y_i)$ are phase averaged and the parameter a is computed at each phase using the method of maximum likelihood. The variance of the velocity measurements in the viscous sublayer is due (1) to non deterministic reproducibility of the waves, (2) to Doppler noise, (3) to the effects of low data rate. The Doppler noise has been evaluated acquiring the UDVP

signal in water at rest, with a concentration of the tracers and a configuration of the electronic similar to those used during the tests. The low data rate and the fact that the time lasted between to velocity profiles is not an integer fraction of the wave period introduce an error in phase averaging. The phase average is performed at phase φ_i considering the nearest profile at time $\varphi_i\ T/2\pi + nT$ for $n = 0,1,\ldots N$, with a maximum time shift equal to half the time resolution, $t_s \cong 0.02$ s. The computation was carried out at each phase evaluating (1) the variance of the velocity measurements; (2) the parameter a and the friction velocity u_* considering up to 8 points at increasing distance from the bottom. The number of fitting points was chosen with iterative check against the maximum depth of the viscous sub-layer ($yu_*/\nu < 8$).

The temporal variation of the bottom stress may be expressed as:

$$\tau_b = \rho |u_*(t)| u_*(t) \tag{10}$$

where ρ is the fluid density and u_* is the friction velocity. The bottom stress can be related to the water depth averaged horizontal velocity through the friction coefficient:

$$\rho |u_*(t)| u_*(t) = \frac{1}{2} f \rho |U_{av}(t)| U_{av}(t) \tag{11}$$

The data points closest to the wall have a wall distance between 0.26 and 1.6 wall units. The results are reported in Figure 7 only for the aerated bore with period $T = 2.5$ s. Similar results have been obtained for the other two wave periods.

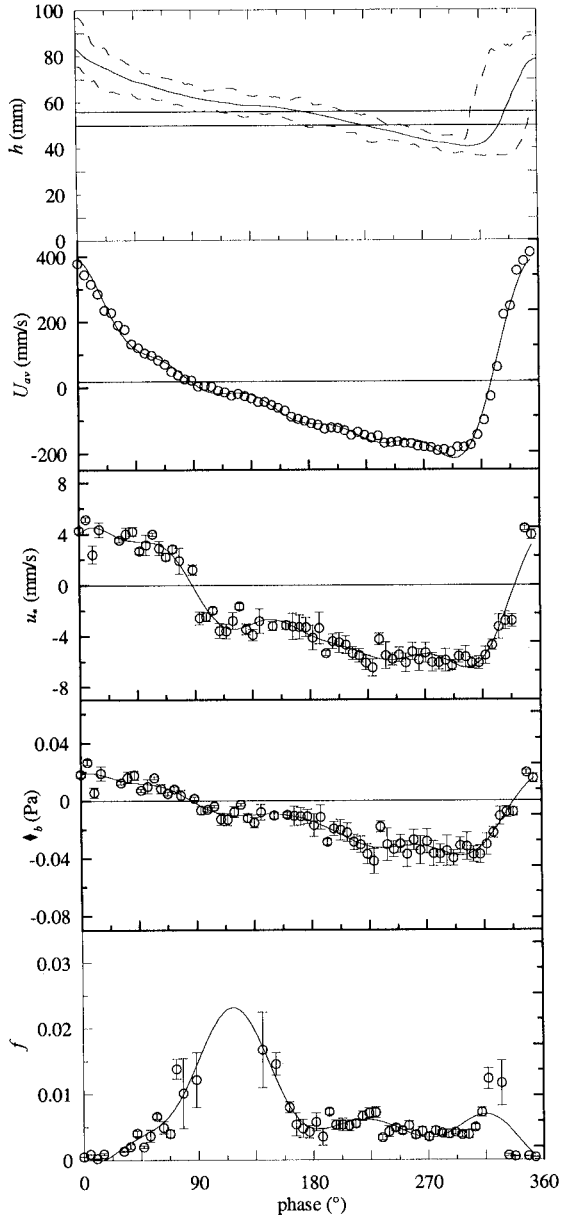

Figure 7. Section B (bore moving region). Depth average horizontal velocity, friction velocity and bottom stress. $T = 2.5$ s.

5. Conclusion

The Empirical Mode Decomposition in Intrinsic Mode Functions and the Hilbert spectrum of those Functions offer a new method for non-linear non-stationary data analysis.

The cross-correlation of the free surface level and of the fluid velocity indicates the frequencies of maximum coupling of the two processes. The computation of the time delay of the maximum cross-correlation could also indicate the celerity of transmission of the information in those cases where the driving process is known. EMD is a good candidate as an efficient tool to clarify the mutual interactions between free surface and the turbulence beneath.

Velocity profiles have been measured on a plexiglas bottom, in a region where velocity profile is linear at least at moderate friction velocity. The measurements in the viscous sub-layer permit the estimation of the bottom stress. With a proper choice of the transducers, velocity measurements very near to the bottom are possible using UltraSounds and the instrument is especially suitable for measurements in the boundary layer.

Acknowledgments

The present work is undertaken as part of Italy-Spain Co-operation Project 1999-2000, funded by MURST of Italy and of Spain

The Software for computing IMFs and for HHT was obtained by NASA under a Software Use Agreement.

References

Huang, N.E., Shen, Z., Long, S.R., Wu, M.C., Shih, H.H., Zheng, Q., Yen, N.-C., Tung, C.C. & Liu, H.H., 1998. The empirical mode decomposition and the Hilbert spectrum for nonlinear and non-stationary time series analysis. Proc. Roy. Soc. London A 454, 903-995.

Kikura, H., Yamanaka, G. and Aritomi, M., 2004. Effect of measurement volume size on turbulent flow measurement using ultrasonic Doppler method. Exp. in Fluids 36, 187-196.

Longo, S. Air bubble effects on Ultrasoundvelocity measurements. (submitted)

Longo, S., Losada, I.J., Petti, M., Pasotti, N. & Lara J., 2001. Measurements of breaking waves and bores through a USD velocity profiler. Technical Report UPR/UCa_01_2001, University of Parma, University of Santander.

Nikora, V.I. and Goring, D.G., 1998. ADV measurements of turbulence: can we improve their interpretation?. J. of Hydraulic Engineering, 124, (6), 630-634.